



Label-free Live and Dead Cell Separation Method Using a High-Efficiency Optically-Induced Dielectrophoretic (ODEP) Force-based Microfluidic Platform

Song-Bin Huang¹, Shing-Lun Liu¹, Jian-Ting Li, and Min-Hsien Wu*

Graduate Institute of Biochemical and Biomedical Engineering, Chang Gung University, Taiwan

¹ These authors contributed equally to this work

(Received 23 September 2013; Accepted 7 November 2013; Published on line 1 June 2014)

*Corresponding author: mhwu@mail.cgu.edu.tw

DOI: [10.5875/ausmt.v4i2.302](https://doi.org/10.5875/ausmt.v4i2.302)

Abstract: This study reports an optically-induced dielectrophoretic (ODEP) force-based microfluidic platform for live and dead cell separation and collection. ODEP forces are used to separate the live and dead cells due to their opposite responses to an ODEP force. Combining the flow control in a microfluidic system, the live and dead cells can be separated and subsequently collected in an efficient and effective manner. The operating conditions of the ODEP force for manipulating the live and dead chondrocytes is characterized, and separation performance is experimentally evaluated. Results revealed that an applied voltage of 8 V resulted in a maximum difference of manipulation force for the live (49.4 pN) and dead (-20.1 pN) cells. Results of further separation experiments showed that the recovery rate and purity of the isolated live cells was as high as 78.3±6.8 % and 96.4 ±2.2 %, respectively. Overall, the proposed method is found to be particularly valuable for biological research which requires the isolation of highly pure live or dead cells.

Keywords: Microfluidics; Optically induced dielectrophoretic (ODEP) force; Cell separation; Live and dead cells

Introduction

Biological, medical and clinical research frequently requires the isolation of a pure cell population with specific cellular properties from a heterogeneous cell suspension. Currently, a wide variety of cell separation methods are used, primarily approaches based on cellular density, adherence, and antibody binding [1, 2]. However, these conventional cell separation methods might not be suitable to isolate some rare cell species (e.g. stem cells [3], or circulating tumor cells [4]) from limited biological or clinical samples due to their larger scale. This technical issue can be resolved by the use of miniaturized devices for cell separation or sorting.

With recent progress in micro electro-mechanical

system (MEMS) or microfluidic technology, several micro-scale devices have been actively pursued for cell separation [5, 6]. These miniaturized cell separation systems are generally believed to provide several advantages over conventional separation techniques, including low sample consumption, low cost, high efficiency, high portability [7], and improved cell separation performance [5-7]. Reports in the literature have demonstrated the use of various working principles in microfluidic systems for cell separation, including size- [8], fluorescence- [9], magnetic- [10], or cell adhesion- [11] based cell separation schemes. Among these, the incorporation of dielectrophoretic (DEP) force-based cell manipulation techniques in microfluidic systems has attracted considerable interest for various cell separations [12]. When microparticles with dielectric



properties (e.g., biological cells) are subjected to a given electric field, charges can be electrically polarized on the particle surface. The interaction between the induced charges on the particles and the applied electric field can generate DEP force [12]. Therefore, by fine-tuning the applied electric field, the microparticles can be manipulated in a manageable manner.

However, DEP force-based cell separation normally requires a costly, time-consuming and technically-demanding microfabrication process to create a unique, application-specific metal electrode layout. Recently, optically-induced dielectrophoretic (ODEP) schemes, in which light images are used as virtual electrodes to induce DEP force, have been actively proposed to manipulate biological cells for various applications [13-19]. The working principle of ODEP force-based cell manipulation is schematically illustrated in Figure 1 (a). Structurally, an ODEP system normally consists of a top indium-tin-oxide (ITO) glass substrate and a bottom ITO glass substrate coated with a photoconductive layer (e.g., amorphous silicon [13-16, 19]). First, an alternating current (AC) voltage is applied between the top and bottom ITO layers to produce a uniform electric field in the system. When the system's photoconductive layer is illuminated, the projected light can excite its electron-hole pairs, and therefore substantially decrease the electrical impedance of the illuminated area. As a result, the applied voltage drops across the liquid layer to the illuminated area, and induces a non-uniform distribution of an electric field between the top and bottom layers. In ODEP force-based cell manipulation, the generated non-uniform electric field is used to manipulate electrically polarised cells [13-19]. Based on this, the cells can be simply manipulated through the optical images illuminated on the photoconductive layer. In operation, one can use a commercial digital projector

to display optical images on a photoconductive material. This allows researchers to quickly modify the electrode setup, thus contributing to a more flexible manipulation of cells as opposed to with the DEP counterpart.

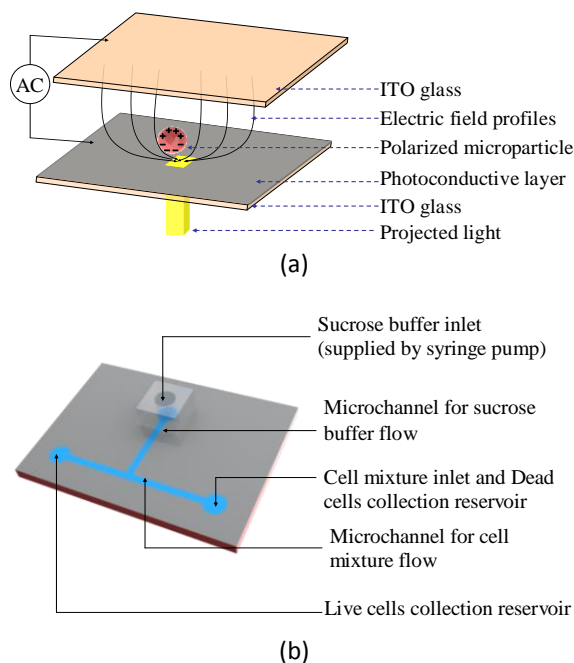


Figure 1. (a) Schematic illustration of the ODEP force generation mechanism, (b) top-view layout.

ODEP force-based cell manipulation has been reported to separate cells with different cellular properties, such as viable and unviable sperm [17], normal and abnormal oocytes [15], different sized cells [16], and high/low quality embryos [18]. However, these studies failed to provide an efficient cell separation scheme to separate the target cells from other unwanted cells, nor did they provide an effective method by which to collect the separated cells. To address the above issues, we propose combining a new microfluidic-based flow control with ODEP-based cell manipulation to achieve both efficient and effective separation and collection of live and dead cells. This study designed and fabricated an ODEP-based microfluidic platform for live and dead cell separation. The operating conditions of ODEP (e.g. magnitude of applied AC voltage) for the manipulation of live and dead chondrocytes were then investigated. Based on the previously-mentioned studies, suitable operating conditions of ODEP were set to separate live and dead chondrocytes in a microfluidic system. Experimental results showed that the proposed cell separation scheme was able to isolate live cells from dead cells with a high recovery rate ($78.3 \pm 6.8\%$) and high purity ($96.4 \pm 2.2\%$). Overall, the proposed cell separation method was found to be particularly valuable for biological research which requires the isolation of highly pure live or dead cells.

Song-Bin Huang received his Ph.D. from the Department of Engineering Science at National Cheng Kung University, Taiwan in 2010. He is currently a postdoctoral researcher in the Graduate Institute of Biochemical and Biomedical Engineering at Chang Gung University. His research interests lie in biomedical applications for microfluidics, optically-induced dielectrophoresis, circulating tumor cells and 3-D cell cultures.

Shing-Lun Liu received his M.S. from the Department of Biomedical Engineering at National Cheng Kung University in 2011. He is currently a researcher assistant at the Graduate Institute of Biochemical and Biomedical Engineering at Chang Gung University, Taiwan. His research interests lie in biomedical applications for microfluidics and dielectrophoresis.

Jain-Ting Li is currently a M.S. student at the Chang Gung University. His research interests lie in biomedical applications for microfluidics.

Min-Hsien Wu received his Ph.D. from the Department of Engineering Science at the University of Oxford, UK in 2005. He is currently Associate Professor in the Graduate Institute of Biochemical and Biomedical Engineering at Chang Gung University, Taiwan. His research has mainly focused on cartilage tissue engineering, microfluidic technology and bio-sensing.



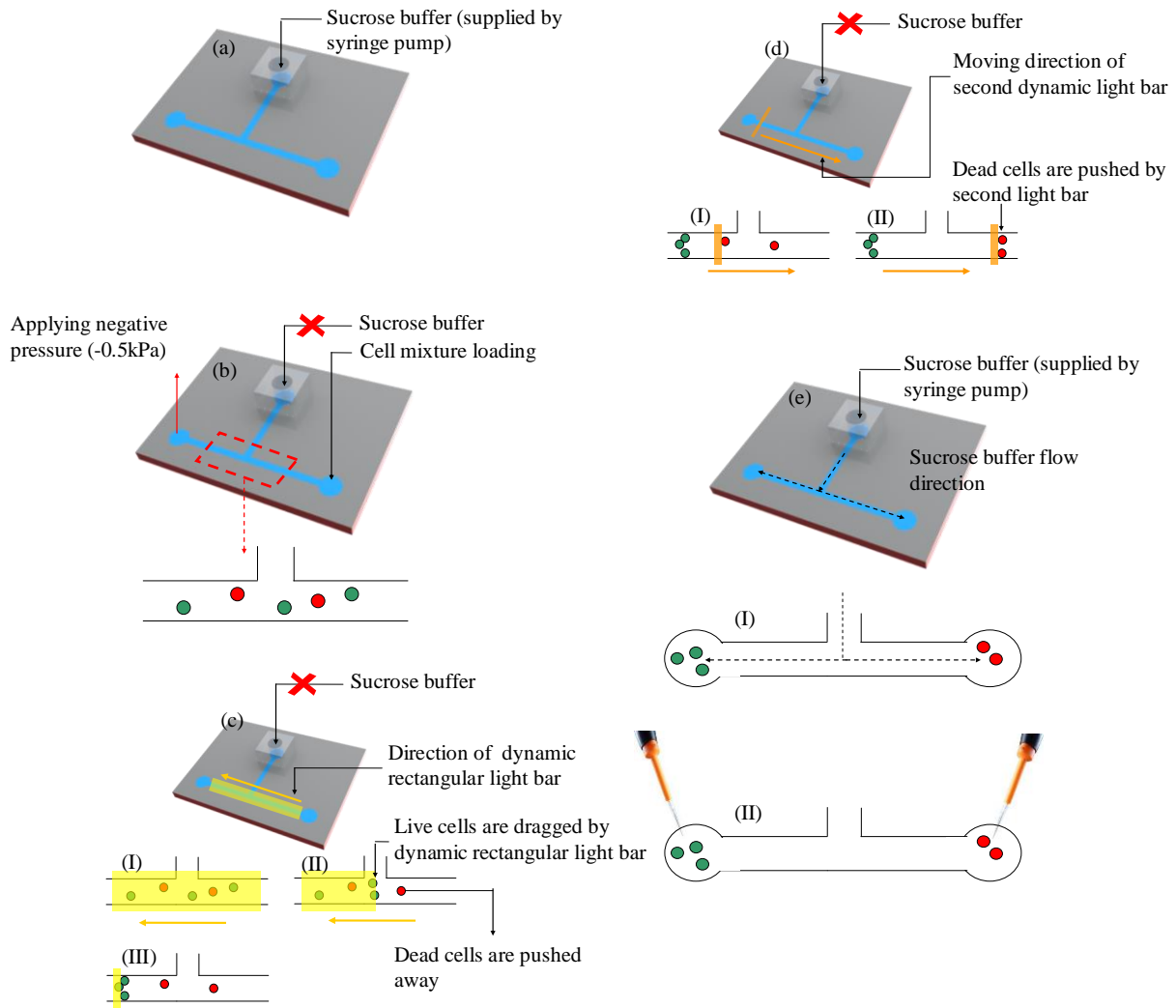


Figure 2. The working mechanism for live and dead cell separation: (a) sucrose solution is loaded into the T microchannel, (b) negative pressure is applied to drive the cell suspension flow, (c) ODEP force is exerted on the microchannel to drive cell mixture flow: (c)-(I) a rectangular light bar is illuminated on the microchannel and, (c)-(II)-(III) dynamic shrinkage of the rectangular light bar to one direction so as to gather the live cells, (d) another dynamic light bar moves in the opposite direction to collect the dead cells, and (e) sucrose solution is delivered into the T microchannel to drive the separated live and dead cells to their respective collection reservoirs.

Materials and methods

Design and principle

An efficient and effective operation scheme for ODEP force-based cell manipulation is proposed to separate live and dead cells in a microfluidic system with a T-shaped microchannel, as illustrated in Figure 1 (b). In the T-shaped microchannel, one microchannel (L: 15 mm, W: 0.5 mm, H: 50 μ m) is for sucrose solution flow and the other (L: 20 mm, W: 0.5 mm, H: 50 μ m) is for cell mixture flow. ODEP force-based cell manipulation separates the live and dead cells in the latter channel. The separation mechanism is schematically shown in Figure 2. A syringe pump was used to fill the T-shaped microchannel with a sucrose solution (250 mM with 0.5%

BSA, Sigma, Taiwan). The cell mixture sample containing live and dead cells was then loaded to the microchannel for cell mixture flow. A negative pneumatic pressure (-0.5 kPa) was applied at one port to distribute the cell mixture in the microchannel (Figure 2 (b)). After that, a dynamic rectangular light bar was illuminated on the microchannel to exert ODEP force on the loaded cells (Figure 2 (c)). The dynamic shrinkage of the light bar only attracted the live cells towards the shrinking direction of the light bar while simultaneously repelling the dead cells. After this, another dynamic light bar was illuminated moving in the opposite direction to repel and collect the dead cells (Figure 2 (d)). After the two cell populations in the tested sample were partitioned, the sucrose solution was again delivered (flow rate: 0.1 μ l/min) into the T-shaped microchannel to drive the

separated live and dead cells to their respective collection reservoirs (D: 2.0 mm, H: 1.1 mm) (Figure 2 (e)). Thus, the live and dead cells in the sample can be effectively and efficiently separated.

Fabrication and experimental setup

The assembly of the microfluidic system is schematically illustrated in Figure 3 (a). The system consists of a top PDMS substrate (Layer A), an indium-tin-oxide (ITO) glass substrate (Layer B), an adhesive tape with microfabricated T-shaped microchannels (Layer C, thickness: 50 μm), and a bottom ITO glass substrate with a coating layer of photoconductive material (encompassing a 10-nm-thick molybdenum layer, and a 1- μm -thick hydrogenated amorphous silicon layer) (Layer D). Structurally, the reservoir for the sucrose solution is in Layer A. The Layer B contains 2 through holes, functioning as reservoirs for collecting cells.

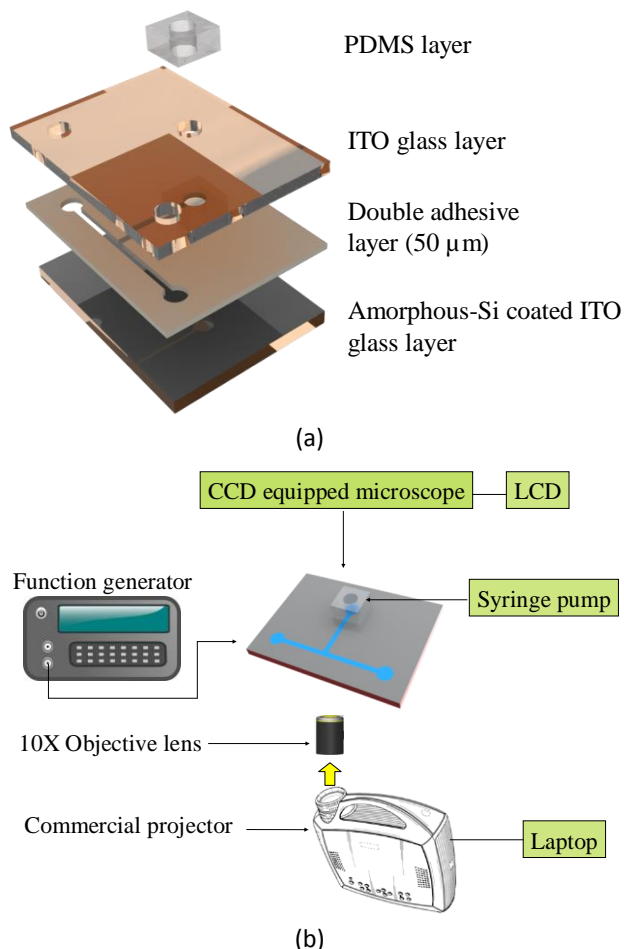


Figure 3. (a) The structure of the proposed microfluidic system for live and dead cell separation, and (b) the overall experimental setup.

The overall fabrication process was based on a computer-numerical-controlled (CNC) and a CO₂ laser micromachining process, a polydimethylsiloxane (PDMS) replica molding, a thin-film technology produced by

sputtering and plasma-enhanced chemical vapour deposition (PECVD), and a plasma oxidation-aided bonding process as described previously [14, 19]. The top PDMS layer (Layer A) (Figure 3 (a)) was fabricated through a combination of CNC machining and PDMS replica molding. For the preparation of the ITO glass substrate (Layer B), 2 through-holes were mechanically drilled in an ITO glass substrate (15 Ω , 1.1 mm; Ritek, Taiwan) using a glass drill. For Layer C, the hollow structure of the T-shaped microchannels was fabricated in a double-sided adhesive tape (9009, 3M, Taiwan) using a CO₂ laser (XS-300, Eurolaser, German). For the bottom substrate (Layer D) (Figure 3 (a)), a 70-nm-thick layer of ITO was sputtered onto a cleaned dummy glass substrate, and treated with a thermal annealing process (240 $^{\circ}\text{C}$, 60 min). A 10-nm-thick molybdenum metal layer was then sputtered onto the ITO layer to reduce contact resistance, thus improving the adhesion between the fabricated ITO glass and the amorphous silicon layer to be deposited subsequently. Based on the PECVD process, a 1- μm -thick amorphous silicon layer was deposited onto the treated ITO glass.

In the subsequent assembly process, Layer A was bonded with Layer B through O₂ plasma treatment. Layer D was then assembled using the fabricated double-sided adhesive tape (Layer C). To achieve the ODEP force-based cell manipulation, a function generator was used to apply an AC voltage between the two ITO glass layers (Layer B and D) (Figure 3 (a)). A commercial digital projector (PLC-XU350, SANYO, Japan) coupled with a laptop computer was used to display controllable light-bars onto the photoconductive material to generate ODEP force on cells. A CCD-equipped microscope (Nikon LV-UEPI 2, Japan) was used to observe the cell separation process. The overall experimental setup is schematically illustrated in Figure 3 (b).

Evaluation of terminal velocity

Terminal velocity is defined as the maximum dragging velocity of a moving light-bar that can manipulate the cells. In this study, such velocity was evaluated by measuring the minimum time required for a moving light-bar to drag a cell a distance of 600 μm under the CCD-equipped microscope [14, 19]. For each cell species (e.g., live and dead chondrocytes) studied, the maximum dragging velocity was experimentally determined for voltages of different magnitudes (2, 4, 6, and 8 V).

Evaluation of cell separation efficiency

Cell separation efficiency was experimentally evaluated. In this study, the fresh primary articular

chondrocytes isolated from the femorotibial joint of 18-24 month old steers were used as the tested cells. The cell isolation process has been well-described previously [14]. The cell suspension obtained was assessed microscopically for cell number and viability using 0.4% (w/v) trypan blue in phosphate buffered saline (PBS; Invitrogen, Taiwan). Only cell preparations with cell viability greater than 95% were used. To preparing the dead cell population, the isolated primary articular chondrocytes were treated with 75% (v/v) alcohol for 20 min. The live and dead cells were then mixed and suspended in 1 ml sucrose solution (solution conductivity: 3.4 $\mu\text{S}/\text{cm}$, permittivity: 78) [19]. The live chondrocytes were observed to have good cell viability in the sucrose solution within 1 hr, which is much longer than the system operation time (about 15 min). In this study, a fluorescent dye kit (LIVE/DEAD1 Viability/Cytotoxicity Kit L-3224, Molecular Probes) was used to identify the live and dead cells [14, 19]. For the evaluation of cell separation efficiency, the prepared cell mixture (2,000 cells containing 50% live and 50% dead chondrocytes in 0.5 μl sucrose solution) was loaded into the chip, and followed by the ODEP force-based cell separation process, as described in Figure 2. The number of the live and dead cells was directly counted through image acquisition software (SimplePCI version 5.2.1, Compix Inc.) [19] to evaluate the recovery rate and purity of live cell isolation. The recovery rate (%), and purity (%) of live cell isolation are respectively defined as the percentage of the isolated live cells over the total number of spiked live cells, and that of number of isolated live cell number over the total number of cells collected.

Results and discussion

Characterization of the operation conditions of ODEP for live and dead chondrocyte manipulation

This study characterizes the operating conditions of ODEP force for manipulating live and dead chondrocytes. In theory, the generated ODEP force acting on cells can be expressed through Equation (1) describing the DEP force:

$$F_{DEP} = 2\pi r^3 \varepsilon_m \text{Re}[K(\omega)] \nabla E^2, \quad (1)$$

where r , ε_m , E , and $K(\omega)$ respectively denote the cell radius, the permittivity of the solution surrounding the cells, the root-mean-square electric field strength, and the real part of the Clausius–Mossotti factor. For the single-shell model [16], the $K(\omega)$ can be described by Equation (2):

$$K(\omega) = \frac{\varepsilon_{cell}^* - \varepsilon_m^*}{\varepsilon_{cell}^* - 2\varepsilon_m^*},$$

$$\varepsilon_{cell}^* = C_{mem}^* \frac{3r\varepsilon_{int}^*}{3\varepsilon_{int}^* + 3C_{mem}^*r}, \quad (2)$$

$$\varepsilon_m^* = \varepsilon_m - j \frac{\sigma_m}{\omega},$$

Where ε_{cell}^* , ε_m^* , σ_m , ω , ε_{int}^* , and C_{mem}^* respectively represent cell permittivity, medium permittivity, medium conductivity, the angular frequency of the electric field, the complex internal conductivity of cells, and cell membrane capacitance.

In reality, however, the forces acting on the manipulated cells were quite complex [14], and could include forces due to dielectrophoresis, AC electroosmosis, thermophoresis, hydrodynamic drag, or friction [14, 19]. In ODEP force-based cell manipulation, it has been reported that the AC electro-osmosis and electro-thermal forces are not significant under the specific voltage conditions (V: 2–7 V, frequency: 100 kHz) [20], and the two forces were thus ignored in this study. Nevertheless, the generated ODEP force attracts the cells toward the surface of the amorphous silicon layer, and thus the friction force should be considered when the light pattern moves to drag or pull the cells. To simplify the forces acting on the cells, one could define the manipulation force, which as a net force between the ODEP force and the friction force [14, 19]. In a steady state, the manipulation force was balanced by the viscous drag of the fluid, which was related to the velocity of a spherical particle by Stokes' law. Hence, the hydrodynamic drag force could be used to evaluate the net manipulation force [14, 19]. Stokes' law describes the drag force (F) exerted on a spherical particle in a continuous flow condition, and can be expressed as Equation (3):

$$F = 6\pi r \eta v, \quad (3)$$

where r , η , and v respectively denote the radius of cells, the viscosity of the fluid, and the terminal velocity of the cells. At a given cell size and viscosity of the surrounding solution, the manipulation force generated under a specific operating condition can be estimated from the terminal velocity of the cells. In this study, the maximum velocity of a moving light-bar dragging or pulling a cell was measured to calculate the manipulation force according to the Stokes' law (Equation (3)), as previously described.

Figure 4 shows the measured terminal velocity (and the calculated manipulation force) of the live and dead chondrocytes under different magnitudes of applied voltage (2, 4, 6, and 8 V). For the live

chondrocytes, the terminal velocity (and manipulation force) increased with the applied voltage. The results in Figure 4 agree with Equation (1), showing that the force is proportional to the voltage squared. Within the experimental conditions explored, the maximum manipulation force was produced with the application of 8 V of AC voltage at 50 kHz. However, the exerted ODEP force not only attracted the live cells but also repelled the dead cells under the sample operation conditions. This phenomenon can be explained by Equation (2). In the microchannel, the cells were suspended in the sucrose solution with a level of conductivity significantly less than that of a viable cell [21]. Under this circumstance, the live cells were highly polarized in a given electric field and thus induced more dipole moment. This caused the cellular complex internal conductivity (C_{mem}^*) of the live chondrocytes to exceed that of surrounding medium (σ_m) and resulted in a significant electric gradient, thus the live chondrocytes tended to be attracted by the ODEP electrical field [13, 17]. Conversely, the dead chondrocytes could not maintain an ionic gradient across their membranes and organelles due to the loss of membrane integrity. They were only weakly polarized by the ODEP electrical field leading to a repulsive response to the ODEP electrical field as reported previously [17]. The above might explain the positive (live cells) and negative (dead cells) ODEP forces found in this investigation (Figure 4). Based on above phenomenon, overall, one can simply use the ODEP forces to separate the live and dead cells due to their opposite response to an ODEP field. From Figure 4, the applied voltage condition of 8 V was chosen for the cell separation due to the maximum difference of manipulation force for the live (49.4 pN) and dead (-20.1 pN) cells.

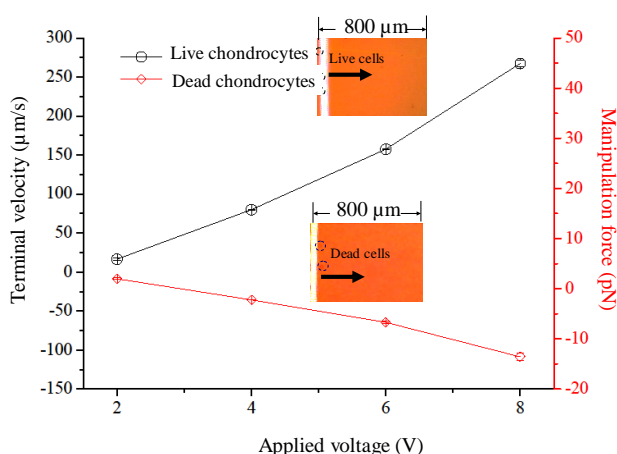


Figure 4. Evaluation of the terminal velocity and the manipulation force of the live and dead chondrocytes under different magnitudes of applied voltage (2, 4, 6, and 8 V).

Performance of live chondrocytes isolation using the ODEP force-based microfluidic platform

To demonstrate the feasibility of using the proposed method for live and dead cell separation, experimental investigations were carried out. Figure 5 (a) shows sequential microscopic images of the all procedures for live and dead chondrocyte separation and collection. First, a dynamic rectangular light bar with 267.2 µm/s in moving velocity was designed to drag the live chondrocytes (Figure 5 (a)-(c)) to the live cell collection reservoir side of the microchannel, while simultaneously repelling and excluding the dead cells (Figure 5 (c)-(e)). After the live chondrocytes were clustered to the side near the live cell collection reservoir (refer to Figure 1 (b)), another dynamic light bar moving in the opposite direction pulled and collected the dead cells to the side near the dead cell collection reservoir (Figure 5 (g)-(h)). Through this two-step process the two cell populations can be efficiently and effectively separated as shown in Figure 5 (i). After the two chondrocyte populations in the tested sample were partitioned, the sucrose solution was again pumped into the T-shaped microchannel to drive the separated live and dead chondrocytes to their respective collection reservoirs. Figure 6 (a) shows the fluorescent microscopic images of the separated live and dead chondrocyte populations. Figure 6 (b) shows the recovery rate and purity of the isolated live cells respectively reach 78.3±6.8 % and 96.4 ±2.2 %. This suggests that the proposed method achieves a high recovery rate and good separation of live and dead cells.

Conclusion

The combination of ODEP force-based cell manipulation and the flow control in a microfluidic system was successfully used to separate and then collect live and dead cells. In the study, positive and negative ODEP forces were used to separate the two cell populations under a given ODEP force background. An applied voltage of 8 V produced the maximum difference of manipulation force for the live (49.4 pN) and dead (-20.1 pN) cells. Performance evaluation showed that the recovery rate and purity of the isolated live cells reached 78.3±6.8 % and 96.4 ±2.2 %, respectively. The proposed operation scheme could prove particularly valuable for biological research requiring the precise isolation of live or dead cells.

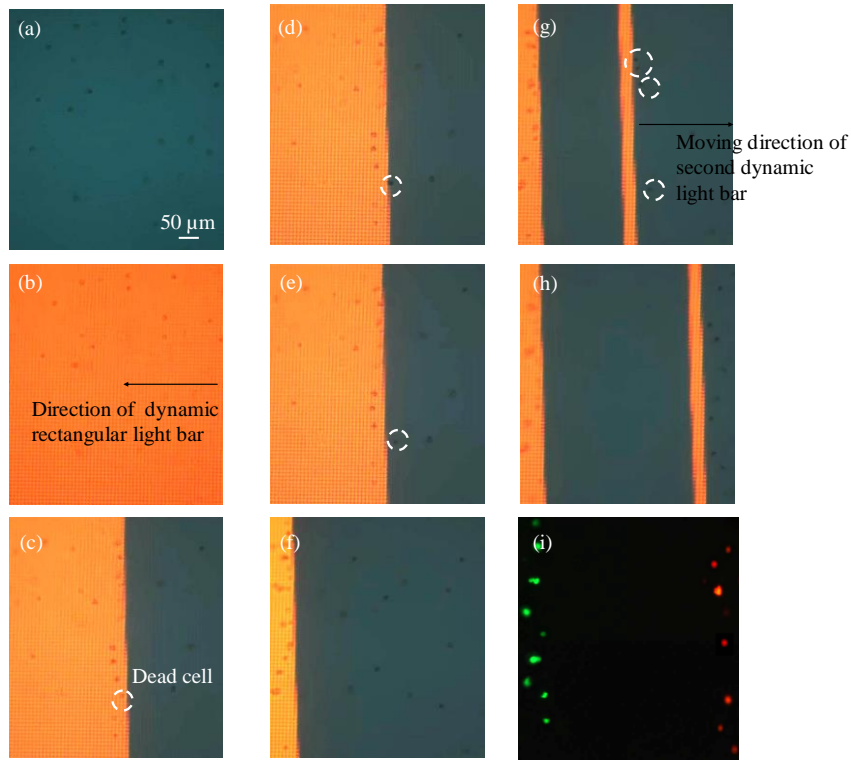


Figure 5. Microscopic observation of the sequential actions for live and dead cell separation: (a) the original state, (b) the illumination of the rectangular light bar on the microchannel to generate ODEP force on the cells, (c)-(f) the dynamic shrinkage of the light bar so as to gather the live cells to one side, (g)-(h) the illumination of another dynamic light bar to collect the dead cells, and (i) the fluorescent microscopic images of the separated cells, in which the green and red dots respectively represent the live and dead cells.

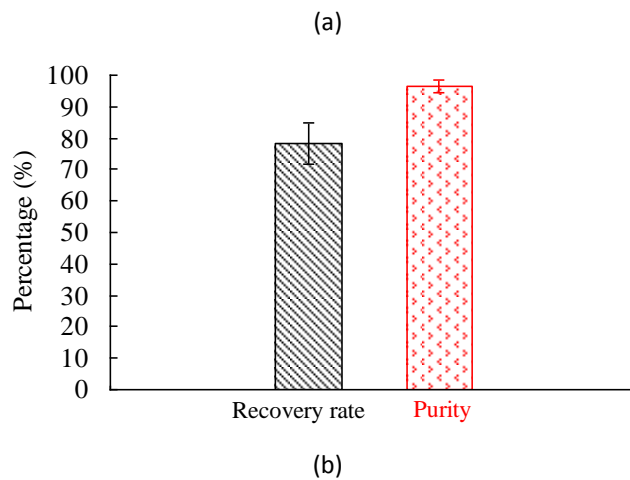
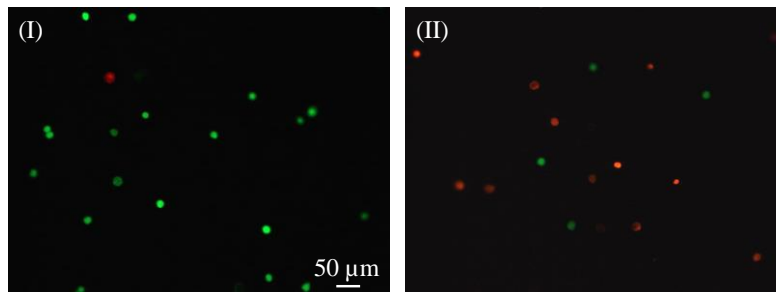


Figure 6. (a) Fluorescent microscopic images of the separated (I) live and (II) dead cell populations, in which the green, and red dots respectively represent the live and dead cells, and (b) evaluation of the recovery rate and purity of the isolated live cells.

Acknowledgement

This project was sponsored by the Chang Gung Memorial Hospital (CMRPD2C0101).

References

- [1] L. M. Wahl, I. M. Katona, R. L. Wilder, C. C. Winter, B. Haraoui, I. Scher, and S. M. Wahl, "Isolation of human mononuclear cell subsets by counterflow centrifugal elutriation (cce): I. Characterization of b-lymphocyte-, t-lymphocyte-, and monocyte-enriched fractions by flow cytometric analysis," *Cellular Immunology*, vol. 85, no. 2, pp. 373-383, 1984.
doi: [10.1016/0008-8749\(84\)90251-X](https://doi.org/10.1016/0008-8749(84)90251-X)
- [2] M. Hristov, W. Erl, and P. C. Weber, "Endothelial progenitor cells: Isolation and characterization," *Trends Cardiovasc Med*, vol. 13, no. 5, pp. 201-206, 2003.
doi: [10.1016/S1050-1738\(03\)00077-X](https://doi.org/10.1016/S1050-1738(03)00077-X)
- [3] R. B. Clarke, "Isolation and characterization of human mammary stem cells," *Cell Prolif*, vol. 38, no. 6, pp. 375-386, 2005.
doi: [10.1111/j.1365-2184.2005.00357.x](https://doi.org/10.1111/j.1365-2184.2005.00357.x)
- [4] M. Yu, S. Stott, M. Toner, S. Maheswaran, and D. A. Haber, "Circulating tumor cells: Approaches to isolation and characterization," *J Cell Biol*, vol. 192, no. 3, pp. 373-382, 2011.
doi: [10.1083/jcb.201010021](https://doi.org/10.1083/jcb.201010021)
- [5] D. R. Gossett, W. M. Weaver, A. J. Mach, S. C. Hur, H. T. Tse, W. Lee, H. Amini, and D. Di Carlo, "Label-free cell separation and sorting in microfluidic systems," *Anal Bioanal Chem*, vol. 397, no. 8, pp. 3249-3267, 2010.
doi: [10.1007/s00216-010-3721-9](https://doi.org/10.1007/s00216-010-3721-9)
- [6] A. Lenshof and T. Laurell, "Continuous separation of cells and particles in microfluidic systems," *Chemical Society Reviews*, vol. 39, no. 3, pp. 1203-1217, 2010.
doi: [10.1039/B915999C](https://doi.org/10.1039/B915999C)
- [7] S. K. Sia and G. M. Whitesides, "Microfluidic devices fabricated in poly(dimethylsiloxane) for biological studies," *Electrophoresis*, vol. 24, no. 21, pp. 3563-3576, 2003.
doi: [10.1002/elps.200305584](https://doi.org/10.1002/elps.200305584)
- [8] T. Laurell, F. Petersson, and A. Nilsson, "Chip integrated strategies for acoustic separation and manipulation of cells and particles," *Chem Soc Rev*, vol. 36, no. 3, pp. 492-506, 2007.
doi: [10.1039/b601326k](https://doi.org/10.1039/b601326k)
- [9] D. Huh, W. Gu, Y. Kamotani, J. B. Grotberg, and S. Takayama, "Microfluidics for flow cytometric analysis of cells and particles," *Physiol Meas*, vol. 26, no. 3, pp. R73-98, 2005.
doi: [10.1088/0967-3334/26/3/r02](https://doi.org/10.1088/0967-3334/26/3/r02)
- [10] M. A. M. Gijs, "Magnetic bead handling on-chip: New opportunities for analytical applications," *Microfluidics and Nanofluidics*, vol. 1, no. 1, pp. 22-40, 2004.
doi: [10.1007/s10404-004-0010-y](https://doi.org/10.1007/s10404-004-0010-y)
- [11] W. C. Chang, L. P. Lee, and D. Liepmann, "Biomimetic technique for adhesion-based collection and separation of cells in a microfluidic channel," *Lab Chip*, vol. 5, no. 1, pp. 64-73, 2005.
doi: [10.1039/b400455h](https://doi.org/10.1039/b400455h)
- [12] Z. R. Gagnon, "Cellular dielectrophoresis: Applications to the characterization, manipulation, separation and patterning of cells," *Electrophoresis*, vol. 32, no. 18, pp. 2466-2487, 2011.
doi: [10.1002/elps.201100060](https://doi.org/10.1002/elps.201100060)
- [13] P. Y. Chiou, A. T. Ohta, and M. C. Wu, "Massively parallel manipulation of single cells and microparticles using optical images," *Nature*, vol. 436, no. 7049, pp. 370-372, 2005.
doi: [10.1038/nature03831](https://doi.org/10.1038/nature03831)
- [14] Y. H. Lin, Y. W. Yang, Y. D. Chen, S. S. Wang, Y. H. Chang, and M. H. Wu, "The application of an optically switched dielectrophoretic (odep) force for the manipulation and assembly of cell-encapsulating alginate microbeads in a microfluidic perfusion cell culture system for bottom-up tissue engineering," *Lab Chip*, vol. 12, no. 6, pp. 1164-1173, 2012.
doi: [10.1039/c2lc21097e](https://doi.org/10.1039/c2lc21097e)
- [15] H. Hwang, D. H. Lee, W. Choi, and J. K. Park, "Enhanced discrimination of normal oocytes using optically induced pulling-up dielectrophoretic force," *Biomicrofluidics*, vol. 3, no. 1, p. 014103, 2009.
doi: [10.1063/1.3086600](https://doi.org/10.1063/1.3086600)
- [16] A. T. Ohta, P. Y. Chiou, H. L. Phan, S. W. Sherwood, J. M. Yang, A. N. K. Lau, H. Y. Hsu, A. Jamshidi, and M. C. Wu, "Optically controlled cell discrimination and trapping using optoelectronic tweezers," *IEEE Journal of Selected Topics in Quantum Electronics*, vol. 13, no. 2, pp. 235-243, 2007.
doi: [10.1109/JSTQE.2007.893560](https://doi.org/10.1109/JSTQE.2007.893560)
- [17] M. M. Garcia, A. T. Ohta, T. J. Walsh, E. Vittinghof, G. Lin, M. C. Wu, and T. F. Lue, "A noninvasive, motility independent, sperm sorting method and technology to identify and retrieve individual viable nonmotile sperm for intracytoplasmic sperm injection," *J Urol*, vol. 184, no. 6, pp. 2466-2472, 2010.
doi: [10.1016/j.juro.2010.08.026](https://doi.org/10.1016/j.juro.2010.08.026)
- [18] J. K. Valley, P. Swinton, W. J. Boscardin, T. F. Lue, P. F. Rinaudo, M. C. Wu, and M. M. Garcia, "Preimplantation mouse embryo selection guided by light-induced dielectrophoresis," *PLOS ONE*, vol. 5, no. 4, p. e10160, 2010.
doi: [10.1371/journal.pone.0010160.g001](https://doi.org/10.1371/journal.pone.0010160.g001)



- [19] S. B. Huang, M. H. Wu, Y. H. Lin, C. H. Hsieh, C. L. Yang, H. C. Lin, C. P. Tseng, and G. B. Lee, "High-purity and label-free isolation of circulating tumor cells (ctcs) in a microfluidic platform by using optically-induced-dielectrophoretic (odep) force," *Lab Chip*, vol. 13, no. 7, pp. 1371-1383, 2013.
doi: [10.1039/c3lc41256c](https://doi.org/10.1039/c3lc41256c)
- [20] J. K. Valley, A. Jamshidi, A. T. Ohta, H. H. Yin, and M. C. Wu, "Operational regimes and physics present in optoelectronic tweezers," *Journal of Microelectromechanical Systems*, vol. 17, no. 2, pp. 342-350, 2008.
doi: [10.1109/JMEMS.2008.916335](https://doi.org/10.1109/JMEMS.2008.916335)
- [21] S. W. Dessie, F. Rings, M. Holker, M. Gilles, D. Jennen, E. Tholen, V. Havlicek, U. Besenfelder, V. L. Sukhorukov, U. Zimmermann, J. M. Endter, M. A. Sirard, K. Schellander, and D. Tesfaye, "Dielectrophoretic behavior of in vitro-derived bovine metaphase ii oocytes and zygotes and its relation to in vitro embryonic developmental competence and mrna expression pattern," *Reproduction*, vol. 133, no. 5, pp. 931-946, 2007.
doi: [10.1530/rep-06-0277](https://doi.org/10.1530/rep-06-0277)

